A Combined Atomic Force Microscopy and Molecular Dynamics Simulation Study on a Plastocyanin Mutant Chemisorbed on a Gold Surface

Anna Rita Bizzarri, Beatrice Bonanni, Giulio Costantini, and Salvatore Cannistraro*[a]

A mutant of copper plastocyanin, covalently bound to an Au (111) surface through an engineered disulfide bridge, was investigated in aqueous medium by atomic force microscopy (AFM) and molecular dynamics (MD) simulations. Tapping-mode AFM images revealed adsorption of single molecules which are homogeneously distributed over the substrate and strongly bound to gold and display uniform lateral size. A statistical analysis of the height of the macromolecules on the gold substrate evidenced a distribution around a mean value consistent with that expected from the crystallographic data and with a relatively large standard deviation. A 10-ns classical MD simulation of mutated plastocyanin, hydrated by a layer of water, covalently bound to a gold surface by one or two sulfur atoms, was performed. The simulations indicate that the bound protein retains, in both cases, its overall tertiary structure during the dynamic evolution. Moreover, the macromolecule can assume different orientations with respect to the gold substrate, which give rise to a distribution of heights on the gold substrate. Experimental and MD simulation results are compared and discussed in connection with the topological and dynamical properties of the protein system.

Introduction

Full characterisation of the topological and conductive properties of proteins assembled on metal electrodes is an important step in the development and application of bioelectronic devices.[1, 2] Recently, electron transfer (ET) proteins have attracted much attention with regard to building hybrid systems in which their ET properties could be exploited to transduce chemical signals.[3, 4] Copper proteins and their localised redox centres, characterised by a very efficient ET mechanism, have been extensively investigated.[3, 5, 6] In general they are part of ET chains in which conduction through the biomolecule occurs at the single-electron level;[7, 8] such a feature renders these copper proteins promising candidates for the construction of low-dissipation, highly sensitive hybrid monomolecular devices.

In this framework, a mutant of poplar plastocyanin (PC), a copper-containing ET protein involved in photosynthesis, was engineered by introducing a surface disulfide bridge opposite to the active site to allow stable covalent immobilisation on metal electrodes;[9] the resulting mutant (PCSS) was shown to retain the spectroscopic features of the wild-type structure and, likely, the ET properties.[9] Scanning tunnelling microscopy (STM) images of immobilised PCSS at the single-molecule level seem to indicate that the copper active-site is involved in the ET process.[10] In this respect, we note that while lateral dimensions of the macromolecules are well reproduced by STM, the corresponding heights appear to be dramatically lower than expected.[10]

Here we report on investigations on the topological arrangement of PCSS adsorbed on gold substrates under fluid conditions by tapping-mode atomic force microscopy (TMAFM). The TMAFM images recorded from different zones revealed adsorption of single PCSS molecules which are homogeneously distributed over the substrate. The adsorbed proteins appear to be strongly bound to gold and display uniform size that is in agreement with that expected from the crystal structure. A statistical analysis of the TMAFM images indicates that the heights of molecules on the gold substrate are characterised by a monomodal distribution with a rather large width parameter; such behaviour suggests a heterogeneity in the orientation of the macromolecules with respect to the gold substrate.

To gain further insight into the arrangement and orientation of the protein on the gold substrate, its structural and dynamic properties were investigated by MD simulation. In addition, the MD simulation capabilities were exploited to more deeply investigate whether the dynamic response and flexibility of the adsorbed macromolecules could be affected by involving one or

[a] *Prof. S. Cannistraro, Prof. A. R. Bizzarri, Dr. B. Bonanni, Dr. G. Costantini*
Biophysics and Nanoscience Group
INFM, Dipartimento di Scienze Ambientali
Università della Tuscia, Largo dell'Università
01100 Viterbo, Italy
Fax: (+39) 0761-357179
E-mail: cannistr@unitus.it

 DOI: 10.1002/cphc.200300792

both sulfur atoms of the disulfide bridge in anchoring of the protein to the gold substrate.

Starting from the crystallographic structure, the plastocyanin mutant containing a disulfide bridge was allowed to approach a gold substrate modelled by a cluster of three layers in the Au(111) configuration. The adsorption of the mutant PCSS on the gold substrate was described by assuming that, after breaking of the disulfide bridge, one or both of the sulfur atoms are covalently bound to gold. The protein adsorbed on gold was hydrated by a layer of water, and MD simulations were performed for 10 ns. Analysis of a number of significant structural and dynamic properties of protein – gold systems indicates that in both cases the macromolecule has properly equilibrated and preserves its native structure. In addition, it was found that the protein can adopt a variety of orientations with respect to the gold surface. These results were statistically analysed and are discussed in connection with the related experimental data.

Experimental Section

Design, expression and purification of PCSS were carried out as previously reported.[9] The protein integrity and the copper-site properties of PCSS were assessed by extensive spectroscopic and structural characterisation.[9, 11] The redox functionality of PCSS immobilised on a gold electrode was assessed by preliminary cyclic voltammetry experiments.[10]

For the morphological characterisation of PCSS molecules adsorbed on gold substrates we used a Nanoscope IIIa/Multimode scanning probe microscope (Digital Instruments Inc.) equipped with a 12 μm scanner operating in tapping mode (TM). In this configuration the tip is kept oscillating at its resonant frequency (15 – 35 kHz), and the reduction in oscillation amplitude due to tip – surface interaction is used to identify and measure surface features. Thanks to the intermittent contact between tip and sample, frictional forces are drastically reduced compared to contact mode, so that both damage and indentation of soft samples by the tip are minimised.

Commercial sharpened silicon nitride probes (Digital Instruments), 100 or 200 μm long, with nominal radius of curvature of 20 nm and spring constants of 0.15 and 0.57 N m^{-1}, respectively, were used. All protein imaging was performed in buffer solution in the a fluid cell without O-ring seal. Before engaging, scan size and offsets were set to zero to minimise sample deformation and contamination of the tip. Free oscillation of the cantilever was set to have a root-mean-square amplitude corresponding to about 1.5 V. In each measurement, the set point was adjusted before scanning, to minimise the force between the tip and the sample. The typical scan rate was 0.5 Hz.

Gold substrates (from Molecular Imaging) consisted of a vacuum-evaporated thin gold film (thickness 200 nm) deposited on mica. Prior to experiments, substrates were flame-annealed to obtain recrystallised Au(111) terraces. The quality of the annealed gold substrates was monitored by contact-mode AFM measurements in air (not shown here), which confirmed the presence of high-quality recrystallised (111) terraces, a few hundreds of nanometers in size, with a typical roughness of about 0.1 nm. The substrates were incubated at 4 °C with 7 μM protein solution in 20 mM sodium phosphate buffer (pH 6.0) for 1 h. After incubation, samples were gently rinsed with ultrapure water (resistivity 18.2 MΩ cm) to remove weakly adsorbed proteins and covered with 35 μL of buffer solution for immediate fluid imaging. As a control, Au(111) substrates were treated in similar way but without the addition of proteins. They were scanned under identical conditions to ensure that no spurious images were obtained.

Computational Section

The MD simulations were performed with CHARMM[12] version c27 using PARM27 all-atom parameter set.[13] Initial coordinates of PCSS were taken from the X-ray structure, at 0.16 nm resolution, of the mutant poplar PC bearing a disulfide bridge introduced by replacing Ile21 and Glu25 by two cysteine residues (1JXG entry of Brookhaven Protein Data Bank).[11]

Plastocyanin is an eight-stranded antiparallel β-barrel macromolecule in which a copper atom is ligated by the side chains of two histidine (His37 and His87), a cysteine (Cys84) and a methionine (Met92) residue in a peculiar, tetrahedral geometry.[14] With the exception of the copper ligands His37, Cys84 and His87, all the ionisable residues were assumed to be in their fully charged state in accordance with the pH value. As in previous works, a covalent-bond approach for the copper site was adopted.[15–17] In particular, the copper atom was considered bound to three ligands (two N atoms from His37 and His87 and one S atom from Cys84), while the much weaker interaction of copper with the S atom of Met92 was treated by a nonbonded approach.[18]

To model the Au(111) surface, gold atoms were arranged hexagonally in a cluster of three layers, each with 22 × 25 atoms; the charge on the gold atoms was set to zero. The nearest-neighbour distance was assumed to be 2.88 Å, and the positions of the gold atoms were fixed in all simulations. Two possible modes of binding of PCSS to the gold surface were investigated by involving one or both sulfur atoms of the engineered S—S bridge (see Figure 1).[9] In particular, after breaking of the disulfide bridge, it was assumed that one or both sulfur atoms are covalently bound to gold atoms. For the system denoted PCSS-I, the Cys25 S atom was assumed to form a covalent bond with the gold substrate, and the second S atom of the bridge was saturated with a hydrogen atom, as in the standard cysteine configuration. In the configuration denoted PCSS-II, both Cys25 and Cys21 S atoms were covalently anchored to the gold substrate. In both cases, the S atom was bound by three fcc (face centred cubic) hollow-site gold atoms, placed at the centre of the area surface, such a geometrical arrangement having shown to be energetically more favourable.[19] More details on the anchoring procedure are reported in ref. [20]. The parameters used to describe the gold – protein interactions are reported in Table 1.[21]

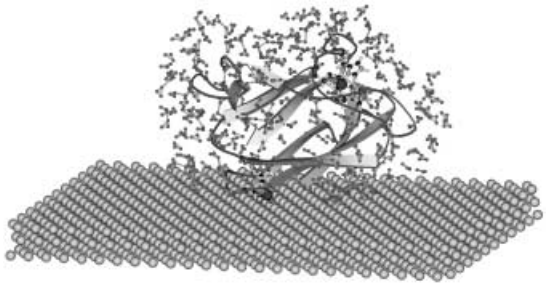

Figure 1. *Visual molecular dynamics (VMD) graphic representation showing PCSS immobilised through the S—S group on an Au(111) substrate. The Cu atom is indicated by the sphere at the top, the S atoms are indicated by smaller spheres at the bottom and the 303 water molecules are represented by small spheres surrounding the molecule. Protein coordinates are from X-ray crystallography.[11]*

Table 1. *Force field parameters describing the interactions between PCSS and the gold surface.[21] These interaction parameters are added to the CHARMM27 all-atoms interactions.*

Interactions	Parameters	
Harmonic bond interaction	r_o [Å]	k_r [kcal mol^{-1} Å^{-2}]
Au – S	2.531	198
S – C	1.836	205
Harmonic angle interaction	θ_o [deg]	k_θ [kcal mol^{-1}]
Au – S – C	109	46.347
Dihedral angle interaction	ϕ_o [deg]	nk_ϕ [kcal mol^{-1}][a]
Au – S – C – C	180	0.312
S – C – C – C	− 19	9.222
Lennard – Jones interaction[b]	r_{min} [Å]	E_{min} [kcal mol^{-1}]
Au	2.0736	0.078

[a] n = multiplicity of the dihedral angles. [b] See ref. [16].

Starting from the initial structure, the protein molecule adsorbed on gold was centred in a cubic box with 5.6568 nm edges and filled with 5832 water molecules equilibrated at 300 K. All water molecules located at a distance from any protein or gold atom of less than 0.280 nm and greater than 0.446 nm for PCSS-I and 0.480 nm for PCSS-II, respectively, were removed; the resulting degree of hydration was about 0.5 g of water per gramme of protein (303 water molecules).

For both systems, 2000 steps of minimization followed by a heating procedure from 0 to 300 K with increments of 5 K every 0.2 ps were performed. Subsequently, an MD simulation at 300 K was carried out for 200 ps with a Gaussian velocity reassignment. Then 10 ns of MD simulation was performed by sampling trajectories at intervals of 0.1 ps. The Shake constraint algorithm[22] was used for all H atoms. Cut-off ratios of 11 and 13 Å were used for the Lennard – Jones and electrostatic energy functions, respectively. The MD simulations were conducted at a constant temperature of 300 K by using the Nose – Hoover method.[23, 24]

Results and Discussion

AFM Measurements

The PCSS proteins likely bind to gold through the disulfide bridge that was inserted by site-directed mutagenesis in a region of the protein opposite to the copper active-site and is readily available for chemisorption onto a gold electrode. Anchoring to gold may involve one or two sulfur atoms.[25] However, in both cases the adsorbed molecule can be schematically represented with the anchoring group facing the gold surface, as in Figure 1.[9, 10]

To characterise the protein morphology and, in particular, the height and the orientation of the macromolecules with respect to the gold substrate, we performed a systematic analysis by TMAFM. All TMAFM images were recorded under fluid conditions (buffer solution) to eliminate capillary forces and minimise height anomalies. These are often present in AFM images recorded in air and are caused by differences in adhesion at the sample surfaces as result of the inhomogeneous thickness of the adsorbed water layer.[26] Since the buffer solution has a pH value close to the isoelectric point for silicon nitride tips,[27] tip – sample interaction is expected to be minimised.

Several TMAFM images have been recorded from different zones of PCSS adsorbed on gold substrates. The topography of PCSS (Figure 2 a) reveals self-assembled molecules homogeneously distributed over the substrate and with uniform lateral size, as was also demonstrated by several images recorded from different areas of the sample (not shown). The proteins appear to be strongly bound to gold, as evidenced by high-quality images

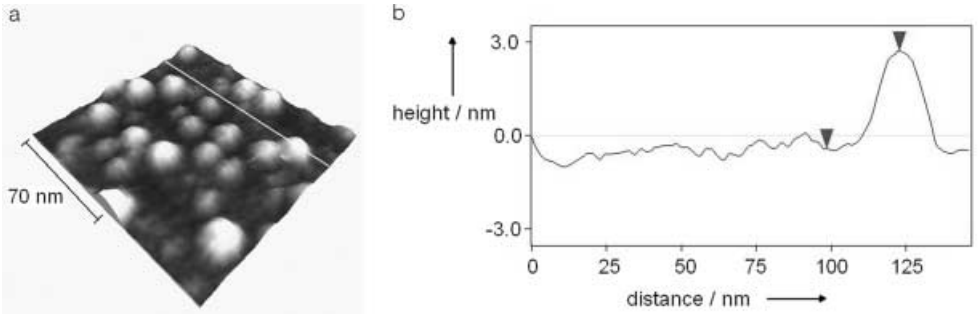

Figure 2. *a) High resolution image of PCSS molecules adsorbed on Au (111), recorded in buffer solution by TMAFM. b) Representative cross-section profile as recorded along the white line in a). Scan area: 145 × 145 nm², vertical range: 8 nm.*

even after repetitive scans. The stability and robustness of binding were evident in STM experiments too, which also gave reproducible images after repetitive scans.[10] Figure 2 shows that individual molecules can be well resolved on the gold surface, as is also observed in STM images (not shown),[10] so that this sample is suitable for statistical analysis of molecular arrangement on the substrate. The typical PCSS lateral dimension, as evaluated from the full width at half maximum of the molecular cross-section profile (Figure 2 b), is in the range 20 – 30 nm. Generally AFM overestimates the diameter of biological samples, due to the relatively large size of the tip and its geometry, which induce broadening effects in the images. The measured lateral dimensions of the protein can be up to five times larger than expected from the crystallographic data. An estimate for the true lateral size of the imaged object can be obtained as follows:[28] for a sherical object and a tip with radius of curvature r, the real diameter d is given approximately by $d = W^2/8r$, where W is the measured apparent width. In our experiment the nominal tip radius is 20 nm and the average apparent width is $W = 25$ nm, so that we obtain for the lateral size of adsorbed PCSS the value $d =$ 3.9 nm, which is close to crystallographic data.[11] Indeed, on the basis of the graphical representation of PCSS anchored to gold by one or both sulfur atoms of the disulfide bridge (Figure 1), one expects from the crystallographic data lateral dimensions of 3.8 × 2.5 nm.[11]

The vertical dimension of the PCSS molecules was estimated, with a resolution of 0.1 nm, from individual cross-section profile analyses (Figure 2b). Data for hundreds of molecules were statistically analyzed, and the results are shown in the histogram of Figure 3. The monomodal distribution is indicative of a preferential orientation of the adsorbed protein molecules on the gold substrate, as expected for specific chemisorption. The mean height is 2.4 nm, with a standard deviation of 0.6 nm. Comparing such dimensions with crystallographic data,[11] the mean height is, within error limits, in agreement with that expected for a nondenaturing immobilisation of proteins on gold through the disulfide bridge ($h = 3.1$ nm).[11]

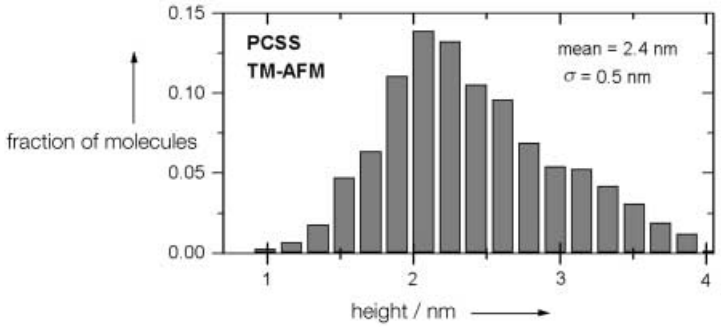

Figure 3. *Statistical analysis of PCSS molecular height on the Au(111) substrate, measured by TMAFM in buffer solution. The vertical dimension of the proteins was estimated from individual cross-section analyses of 742 molecules.*

The standard deviation, which is much larger than the experimental error, is indicative of a significant spread in the vertical size of the molecules. Similar values for the standard deviation of the height were found by other groups in TMAFM imaging of various biomolecules.[4, 29, 30] Generally, the observed spread in the experimental TMAFM data can be attributed to a variety of possible causes. First, even if in tapping mode lateral forces are drastically reduced relative to contact mode, they may be not completely eliminated, and some interactions between the tip and the protein may produce a change in protein orientation. Moreover, if we consider that the tapping frequency is in the kilohertz range, we can expect that even protein movements on the millisecond scale may result in a spread of the measured heights. In addition, a contribution to the observed spread in heights could arise from a heterogeneity in the protein arrangement on the substrate. In this respect, we note that by comparing TMAFM data of PCSS and those of another plastocyanin mutant, with a tail containing a cysteine residue, a different height distribution on the gold substrate was observed.[10] A larger spread in height was observed for this mutant, for which greater protein flexibility is expected.[10] On the other hand, the possibility that PCSS could be anchored to the gold substrate through only one S atom of the disulfide bridge cannot be ruled out (see below).[25]

MD simulations

Although MD simulations are currently employed to investigate the dynamic properties of proteins in connection with experimental approaches,[31–33] only a few attempts have been made to describe the chemisorption of proteins on surfaces[34] and to relate MD simulation with AFM data.[35] The possibility that the dynamics of a protein adsorbed on a bare gold electrode could be reflected in the AFM experimental data have not been investigated.

With the aim of investigating the topological organisation and the dynamic response of a protein covalently bound to a gold electrode, we first analysed a number of properties to assess whether the protein – gold system has properly equilibrated. The root-mean-square displacement (RMSD), from the equilibrated structure, averaged over all the protein atoms, is shown as a function of time in Figure 4 for PCSS-I and PCSS-II . After an initial rise occurring within 100 ps, indicative of the breakdown from the crystallographic structure, both systems reveal a rather stable trend; small oscillations are overimposed on fast fluctuations. Slightly larger RMSD values are registered for PCSS-II than for PCSS-I. This means that by anchoring the macromolecule through two covalent bonds, a larger deviation from the initial structure occurs. However, in both cases, the RMSD values (within the range 0.7 – 0.9 Å) are in good agreement with those generally observed for hydrated proteins[36] and lower than that of wild-type PC (between 1.2 and 1.6 Å).[15] The RMSD values are also generally lower than those determined for PCSS adsorbed on a gold substrate without surrounding water (1.2 – 1.6 Å).[20] Such behaviour suggests that the presence of water of hydration can reduce the perturbation, during the MD simulation, of the protein from the initial

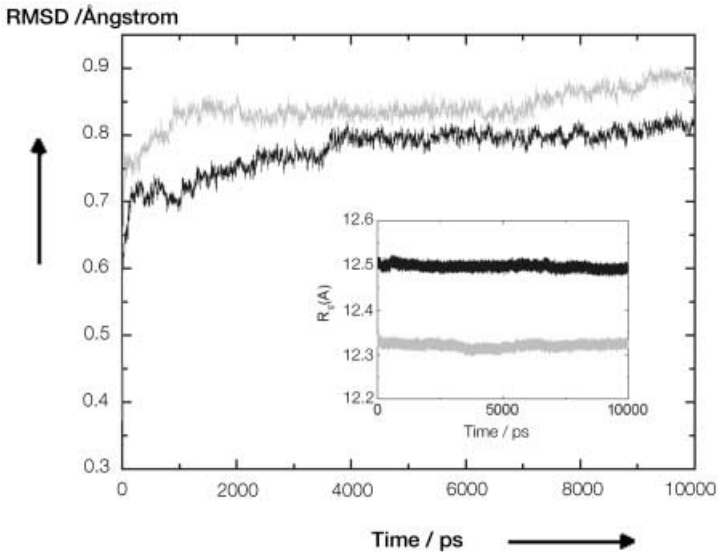

Figure 4. *RMSD from the starting structure of PCSS-I (black) and PCSS-II (grey) along a 10 ns MD simulated trajectory. Inset: gyration ratio of PCSS-I (black) and PCSS-II (grey).*

structure. In this respect, we note that the presence of a single layer of water molecules has been shown to be sufficient to fully activate protein dynamics.[37]

Additional information on the overall dynamic behaviour of the macromolecule during the simulation can be inferred from the trend with time of the gyration ratio R_g (Figure 4, inset). For both systems, R_g is stable over time, in agreement with what was observed in previous simulations of wild-type PC.[15] The reliability of the simulations was further assessed by monitoring the energies during the dynamics. After a short initial time, the potential energies show fast small-amplitude oscillations around a constant mean value, similar to what is observed for fully hydrated wild-type PC.[15]

Now we consider the dynamic properties of the protein with respect to the gold substrate by focussing our attention on the Cu atom relevant for biological functionality. In this regard, the angles θ and ϕ (Figure 5) were analyzed: θ is the angle that the

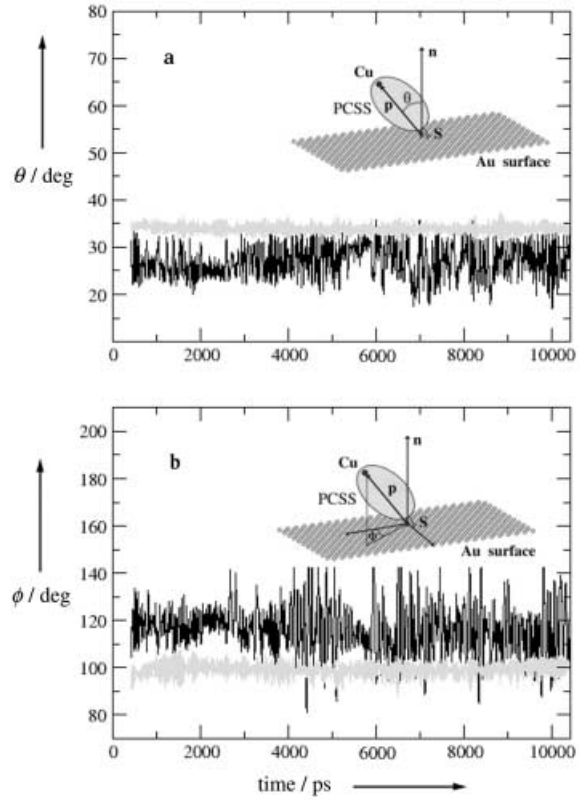

Figure 5. *Temporal evolution, along a 10 ns MD trajectory, of the angles θ (a) and ϕ (b) describing the orientation and the precession, respectively, of the protein p axis with respect to the normal to the gold surface for PCSS-I (black) and PCSS-II (grey). The mean value and the standard deviation of θ are 27 ± 3° and 34 ± 1° for PCSS-I and PCSS-II, respectively. The mean value and the standard deviation of ϕ are 116 ± 10° and 99 ± 3° for PCSS-I and PCSS-II, respectively.*

axis p joining the S atom of Cys25 and the Cu atom forms with the normal n to the gold surface; ϕ is the precession of p about the normal n to the gold surface. The trends with time of θ and ϕ, calculated during the MD trajectory, are plotted in Figure 5 a (PCSS-I) and 5 b (PCSS-II). We note that in both cases a significant deviation of p from the normal axis is registered. In addition, the mean value of θ is smaller for PCSS-I than for PCSS-II (see legend to Figure 5); this means that the protein anchored by a single bond assumes a configuration closer to normal. Such behaviour might be indicative of a less extensive contact between the protein atoms and the gold surface. Furthermore, we note that θ has a larger standard deviation for PCSS-I than for PCSS-II (see legend to Figure 5). Accordingly, the protein anchored to the gold substrate by a single covalent bond appears to be characterised by higher mobility with respect to the gold surface.

Concerning ϕ, PCSS-I and PCSS-II show different average values. Again, a much larger standard deviation is observed for PCSS-I than for PCSS-II (see legend to Figure 5). Such a result, together with what is observed for θ, indicates that the macromolecule, during its dynamic evolution, can assume different arrangements with respect to the gold surface.

These results can provide some hints for interpreting the experimental topological data of immobilised proteins. The protein was represented by an ellipsoid centred at the centre of mass of the protein and oriented according to its main inertial axes. Such an ellipsoid, as evaluated from a snapshot of the macromolecule, provides an overall representation of how the protein is arranged over the substrate (see insets of Figure 5). In this respect, it constitutes a reliable global description of the macromolecule which is appropriate for evaluating its height on the gold substrate. The resulting prolate ellipsoid and its corresponding height on the gold substrate were extracted from the MD simulated trajectories by sampling structures every 10 ps. The histograms of the heights, obtained for 1000 structures, are shown in Figure 6. A monomodal distribution is registered for both systems. The mean values are, in both cases, close to that expected for the crystallographic data by assuming that protein is anchored to gold through the disulfide bridge ($h \approx 3$ nm). On the other hand, we note that PCSS-I has a height mean value slightly higher than that of PCSS-II (see the mean values in Figure 6). Such a finding is consistent with the previous result showing that the protein anchored by a single bond can assume, on average, a configuration closer to the normal to the surface. For both systems, a spread of heights is registered (see the standard deviations in Figure 6). Generally, this means that, during its dynamic evolution, the macromolecule, by exploring its accessible conformations, can assume a variety of arrangements, and hence heights, with respect to the gold substrate. We note that PCSS-I has a wider distribution than PCSS-II. Hence, molecules covalently bound to gold through one S atom show slightly higher flexibility than molecules anchored through two covalent bonds.

Furthermore, the height distributions extracted by MD simulation are markedly narrower than those derived by TMAFM. This could be attributed to the fact that in MD simulation, the observed spread could mainly arise from a variety of orientations sampled by the protein with respect to the gold substrate. In TM-AFM measurements, other effects might contribute to a greater heterogeneity in the height. In particular, the stress exerted by the AFM tip, even in tapping mode, can force the biomolecules into different lateral orientations. Additionally, TMAFM data refer to a collection of molecules, likely in different starting arrange-

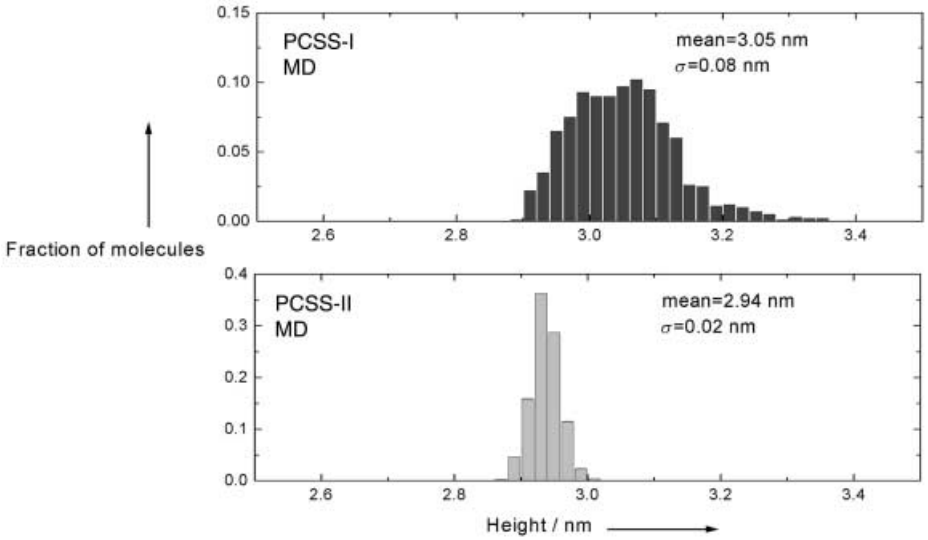

Figure 6. *Statistical analysis of the molecular height on the Au(111) substrate, as extracted from the MD simulated trajectories for PCSS-I and PCSS-II. The vertical dimensions of protein molecules were estimated from 1000 molecules sampled every 10 ps of the MD simulated trajectory.*

ments, which, moreover, may be anchored to gold by one or both S atoms, whereas MD simulations consider only a single molecule and treats the two different modes of anchoring separately.

Considering that TMAFM is sensitive to protein movements on a much longer timescale (at least milliseconds for a tapping frequency in the kilohertz range), it can be hypothesised that the flexibility in such a temporal window of the molecules on the substrate also contributes to the broadening of the experimental height distribution. Finally, the complex interaction between the protein and the gold surface might make a further contribution to the structural and dynamic heterogeneity of the adsorbed protein molecules; such a phenomenon deserves further investigation.

Conclusion

We have presented a conjugated study by AFM and MD simulation of a poplar plastocyanin mutant chemisorbed on gold electrodes through S-containing anchoring groups. To the best of our knowledge our study reports the first MD simulation on a hydrated protein covalently bound to gold. Relating MD simulation and experimental data offers new possibilities for a deeper understanding of how anchoring to gold may affect protein structure and how the dynamics of the adsorbed protein is reflected in the topological properties of the adsorbed protein molecules (height and orientation on the substrate).

The TMAFM images of the mutant PCSS adsorbed on Au(111) show single molecules strongly bound to the gold substrate and with a uniform lateral size that is in agreement with crystallographic data. The molecular height on gold is consistent with the crystallographic values, as expected for nondenaturing adsorption, even though the large spread suggests a significant heterogeneity in the orientation of adsorbed protein molecules.

The MD simulation of PCSS bound to gold surfaces by one or two S atoms shows that the adsorbed protein maintains its native structural properties, consistent with experimental results. The protein dynamics reveals that the macromolecule can assume a variety of arrangements with respect to the gold substrate, which are reflected in a spread of molecular heights on the Au(111) surface. These results provide some hints for interpreting the experimental TMAFM data. Our results suggest that the adsorbed protein on the gold substrate can assume different conformational arrangements that are likely to be detectable experimentally. Due to the two possibilities for anchoring to gold (through one or two S atoms), a larger spread of the vertical size can be expected experimentally with respect to the case in which all protein molecules are anchored to gold in the same way, for instance, as in the MD simulation. In addition, the much longer timescale of TMAFM measurements relative to the restricted temporal window of MD simulations may also account for the broader height distribution observed by AFM compared to MD simulations.

We note that the conjugate approach involving MD simulation and AFM, the potential of which has been only partially explored, could be extremely promising in more closely addressing the topology of biomolecules adsorbed on metal surfaces.

Acknowledgements

We thank Dr. Laura Andolfi for the preparation of the PCSS mutant. This work has been partially supported by the EC Project SAMBA (V Frame FET), the "Molecular Nanodevices" FIRB project and the "Single Molecule Spectroscopy" INFM-PAIS project.

Keywords: chemisorption · metalloproteins · molecular dynamics · scanning probe microscopy · single-molecule studies

[1] I. Willner, B. Willner, *Trends Biotechnol.* **1999**, *121*, 6455.
[2] C. Joachim, J. K. Ginzewski, A. Aviram, *Nature* **2000**, *408*, 541.
[3] J. Zhang, Q. Chi, A. M. Kuznetsov, A. G. Hansen, H. Wackerbarth, H. E. Christensen, J. E. T. Andersen, J. Ulstrup, *J. Phys. Chem. B* **2002**, *106*, 1131.
[4] J. J. Davis, H. A. O. Hill, *Chem. Commun.* **2002**, 393.
[5] H. C. Freeman, J. M. Guss in *Handbook of Metalloproteins*, (Eds.: A. Messerschmidt, R. Huber, K. Wieghardt, T. Poulos), Wiley, Chichester **2001**, pp. 1153 – 1169, 1170 – 1194.
[6] P. Facci, D. Alliata, S. Cannistraro, *Ultramicroscopy* **2001**, *89*, 291.
[7] K. Sigfridsson, M. Ejdeback, M. Sundahl, Ö. Hasson, *Arch. Biochem. Biophys.* **1998**, *351*, 197.

[8] W. Haehnel, T. Jansen, K. Gause, R. B. Klösgen, B. Stahl, D. Michl, B. Huvermann, M. Karas, R. G. Herrmann, *EMBO J.* **1994**, *13*, 1028.
[9] L. Andolfi, S. Cannistraro, G. W. Canters, P. Facci, A. G. Ficca, I. M. C. Van Amsterdam, M. Ph. Verbeet, *Arch. Biochem. Biophys.* **2002**, *399*, 81.
[10] L. Andolfi, B. Bonanni, G. W. Canters, M. Ph. Verbeet, S. Cannistraro, *Surf. Sci.* **2003**, *530*, 181.
[11] M. Milani, L. Andolfi, S. Cannistraro, M. Ph. Verbeet, M. Bolognesi, *Acta Crystallogr.* **2001**, *57*, 1735.
[12] C. L. Brooks, R. E. Bruccoleri, B. D. Olafson, D. J. Statos, S. Swaminathan, M. Karplus, *J. Comput. Chem.* **1983**, *4*, 187.
[13] A. D. MacKerrell, Jr., D. Bashford, M. Bellott, Jr., R. L. Dunbrack, J. D. Evanseck, M. J. Field, S. Fischer, J. Gao, H. Guo, S. Ha, D. Joseph-McCarthy, L. Kuchnir, K. Kuczera, F. T. K. Lau, C. Mattos, S. Michnick, T. Ngo, D. T. Nguyen, B. Prodhom, W. E. Reiher III, B. Roux, M. Schlenkrich, J. C. Smith, R. Stote, J. M. Straub, M. Watanabe, J. Wiorkiewicz-Kuczera, D. Yin, M. Karplus, *J. Phys. Chem. B* **1998**, *102*, 3586.
[14] J. M. Guss, H. D. Bartunik, H. C. Freeman, *Acta Crystallogr.* **1992**, *48*, 790.
[15] A. Ciocchetti, A. R. Bizzarri, S. Cannistraro, *Biophys. Chem.* **1997**, *69*, 185.
[16] L. W. Ungar, N. F. Scherer, G. A. Voth, *Biophys. J.* **1997**, *72*, 5.
[17] A. R. Bizzarri, S. Cannistraro, *Chem. Phys. Lett.* **2001**, *349*, 497.
[18] M. R. Redinbo, T. O. Yeates, S. Merchant, *J. Bioenerg. Biomembr.* **1994**, *26*, 49.
[19] M. C. Vargas, P. Giannozzi, A. Selloni, A. J. Scoles, *J. Phys. Chem. B* **2001**, *105*, 9509.
[20] A. R. Bizzarri, G. Costantini, S. Cannistraro, *Biophys. Chem.* **2003**, *106*, 111.
[21] J. Qian, R. Hentschke, W. Knoll, *Langmuir* **1997**, *13*, 7092.
[22] J. P. Ryckaert, G. Ciccotti, H. J. C. Berendsen, *J. Comput. Phys.* **1977**, *23*, 327.
[23] S. Nose, *J. Chem. Phys.* **1984**, *81*, 511.
[24] W. G. Hoover, *Phys. Rev. A* **1985**, *31*, 1695.
[25] A. Ulman, *Chem. Rev.* **1996**, *96*, 1533.
[26] S. J. T. Van Noort, K. O. Van der Werf, B. G. De Grooth, N. F. Van Hulst, J. Greve, *Ultramicroscopy* **1997**, *69*, 117.
[27] X. Y. Lin, F. Creuzet, H. Arribart, *J. Phys. Chem.* **1993**, *97*, 7272.
[28] J. Vesenka, M. Guthold, C. L. Tang, D. Keller, E. Delain, C. Bustamante, *Ultramicroscopy* **1992**, *42*, 1243.
[29] O. Cavalleri, C. Natale, M. E. Stroppolo, A. Relini, E. Cosulich, S. Thea, M. Novi, A. Gliozzi, *Phys. Chem. Chem. Phys.* **2000**, *2*, 4630.
[30] F. Caruso, D. N. Furlong, K. Ariga, I. Ichinose, T. Kunitake, *Langmuir* **1998**, *14*, 4559.
[31] J. C. Smith, *Q. Rev. Biophys.* **1991**, *24*, 227.
[32] A. Paciaroni, M. E. Stroppolo, C. Arcangeli, A. R. Bizzarri, A. Desideri, S. Cannistraro, *Eur. Biophys. J.* **1999**, *28*, 447.
[33] A. A. Mungikar, D. Forciniti, *ChemPhysChem* **2002**, *3*, 993.
[34] C. E. Nordgren, D. J. Tobias, M. L. Klein, L. K. Blaise, *Biophys. J.* **2002**, *83*, 2906.
[35] M. Rief, H. Grubmüller, *ChemPhysChem* **2002**, *3*, 255.
[36] M.Levitt, R. Sharon, *Proc. Natl. Acad. Sci. USA* **1988**, *85*, 7557.
[37] C. X. Wang, A. R. Bizzarri, Y. W. Xu, S. Cannistraro, *Chem. Phys.* **1994**, *183*, 1.

Received: April 15, 2003 [F 792]

